INTECH
open science | open minds

OPEN ACCESS
ARTICLE

International Journal of Advanced Robotic Systems

Optimal Controller Design of Legless Piezo Capsubot Movement

Regular Paper

Alireza Ahangarani Farahani[1], Amir Abolfazl Suratgar[1,2,*] and Heidar Ali Talebi[1]

1 Department of Electrical Engineering, Amirkabir University of Technology, Tehran, Iran
2 Department of Electrical Engineering, Arak University, Arak, Iran
* Corresponding author E-mail: a-suratgar@aut.ac.ir

Received 9 Jan 2012; Accepted 9 Jun 2012

DOI: 10.5772/51428

Abstract This paper presents an optimal control method based on control effort minimization for a legless piezo capsubot. The capsubot is an underactuated nonlinear dynamics system which is driven by an internal impact force and friction. Here, the motion mechanism of the capsubot is divided into two stages. In the first stage, the aim is to design an optimal controller minimizing energy consumption. In the second stage, optimization is not an objective and instead a four-step strategy for inner mass of the capsubot is proposed. Then, based on the proposed motion strategy, a trajectory profile is given. Using this trajectory profile, the capsubot moves in the desired direction. To evaluate the performance of the proposed control scheme, a comparative study has been performed by means of simulation. Simulation results show that the proposed approach is promising as compared to the Open-Loop Control (OLC) approach and Close-Loop control (CLC) approach which are widely used in the literature for control of capsubots.

Keywords Minimum Effort, Optimal Control, Capsule Robot, Capsubot, Feedback Linearization

1. Introduction

Recently, due to enormous advances in science and technology, autonomous mobile robots have attracted researchers' attention [1], [2], [3]. A capsubot is a type of autonomous mobile robot which can explore fields inaccessible to humans and transmit useful data for analysis [4]. In medical applications, some tiny capsules can be equipped with a miniature camera and can be taken down by the patient to diagnose diseases while causing less pain [5]. In general, two types of capsubots exist: legged capsubots and legless capsubots. The former has an external driving mechanism outside the capsule [6], [7] while the latter is driven by an internal impact force and friction [9], [10]. The disadvantage of the legged capsubot is the complex structure of its mechanism which makes the control difficult in rigorous environments [8]. On the other hand, the legless capsubot has a simple motion structure and can be positioned precisely in a complex environment. While the problem of the design and driving methods of the legless capsubot have received the attention of the researchers, the problem of optimization and control of the legless capsubot has not received the attention it deserves [4]. Optimal control is playing an increasingly important role in the design of modern systems. This method aims to maximize the system efficiency and minimize the predesigned cost function [11].

A seven-step motion strategy in control of capsubot systems is proposed in [4]. With this strategy, three control approaches are investigated: the Open-Loop

Control (OLC) approach, the Closed-Loop Control (CLC) approach using the partial feedback linearization technique and a Simple Switch Control (SSC) approach. Moreover, a variable structure control of a capsubot system is proposed in [5]. In [12], positioning control of a capsubot using sliding mode control is designed because of its robustness to parameter changes. An iterative learning control scheme was designed for a capsubot in [13] and a classic model predictive control approach for a time delay capsubot system is presented in [14] which uses a linearized model for predicting system behaviour. In [15], a four-step acceleration profile for the inner mass of a capsubot system is proposed.

In this paper, the modelling problem of a legless capsubot is investigated. Then optimal control is used to reduce the energy consumption in the capsubot motion. Based on the cost function considered for the optimal control strategy, we can see that less energy is consumed as compared to the OLC and CLC approaches in [4]. In addition, the input force is smoother than the variable structure control in [5], sliding mode control in [12], iterative learning control in [13]and the model predictive control approach in [14].

The remainder of this paper is organized as follows.

Section 2 gives a dynamic model of the capsubot. In Section 3 the motion mechanisms and idea of control are proposed. Controller design is proposed in Section 4. In Section 5 simulation results and the test results are presented. Section 6 concludes the paper.

2. Capsubot dynamics model

The schematic of the capsubot system is shown in Fig.1.

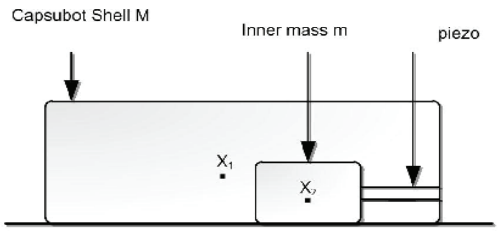

Figure 1. Structure schematic of the legless scapsubot system.

This capsubot has three main parts: the first main part is the capsubot shell with mass M and position x_1, the second main part is the inner mass with mass m and position x_2 and the third main part is the piezoelectric element which generates propulsion force u. This force acts between the capsubot shell and the inner mass. In order to discern the static friction and kinetic friction in the model, two friction parameters are defined, μ_{1s} is the static friction coefficient, μ_{1k} is the kinetic friction coefficient between the capsubot shell and the ground, μ_{2s}represents the coefficient of the static friction, μ_{2k}represents the coefficient of the kinetic friction between the capsubot shell and the inner mass [13].

Using Newton's second law, the following relation is obtained

$$\begin{aligned} &F_M = M\ddot{x}_1 \Rightarrow \\ &u - \mu_{1k}(M+m).g.\text{sign}(\dot{x}_1) \\ &\qquad + \mu_{2k}m.g.\text{sign}(\dot{x}_2 - \dot{x}_1) = M\ddot{x}_1 \end{aligned} \tag{1}$$

The inner mass of the capsubot is obtained in a similar way

$$\begin{aligned} &F_m = m\ddot{x}_2 \Rightarrow \\ &m\ddot{x}_2 + \mu_{2k}mg.\text{sign}(\dot{x}_2 - \dot{x}_1) = -u \end{aligned} \tag{2}$$

where g is the acceleration due to gravity. The argument t in $x(t)$ is dropped for brevity.

Substituting (2) in (1) and rewriting it gives

$$M\ddot{x}_1 + m\ddot{x}_2 + \mu_{1k}(M+m).g.\text{sign}(\dot{x}_1) = 0 \tag{3}$$

Therefore

$$\begin{cases} M\ddot{x}_1 + m\ddot{x}_2 + \mu_{1k}(M+m)g.\text{sign}(\dot{x}_1) = 0 \\ m\ddot{x}_2 + \mu_{2k}mg.\text{sign}(\dot{x}_2 - \dot{x}_1) = -u = \tau \end{cases} \tag{4}$$

The legless capsubot is an underactuated system because it has one control input generated by the piezoelectric part while the legless capsubot has two variables - the capsubot shell position and the inner mass position have to be controlled. Therefore, we obtain the state space equations of the system as

$$\begin{aligned} &x_1 = y_1 \Rightarrow \dot{x}_1 = \dot{y}_1 = y_2, \dot{x}_1 = y_2 \\ &x_2 = y_3 \Rightarrow \dot{x}_2 = \dot{y}_3 = y_4, \dot{x}_2 = y_4 \\ &\begin{cases} \dot{y}_1 = y_2 \\ \dot{y}_2 = -\dfrac{\mu_{1k}}{M}(M+m).g.\text{sign}(y_2) \\ \qquad + \dfrac{\mu_{2k}}{M}m.g.\text{sign}(y_4 - y_2) + \dfrac{1}{M}u \\ \dot{y}_3 = y_4 \\ \dot{y}_4 = -\mu_{2k}g.\text{sign}(y_4 - y_2) - \dfrac{1}{m}u \end{cases} \end{aligned} \tag{5}$$

3. Motion mechanism

In this section, the motion mechanism of the capsubot is presented. Here, the motion mechanism of the capsubot is divided into two stages. In the first stage, the fast backward motion of the inner mass leads to forward motion of the capsubot. In the second stage, the slow forward motion of the inner mass leads to no change in capsubot movement. The aim of this paper is to design an

optimal controller which minimizes energy consumption in the first stage of the motion mechanism.

3.1 Capsubot forward motion mode, $t \in [0; t_2)$

In this stage, the main goal of the capsubot is to move forward. In this mode, two phases are defined.

Phase I: In this phase, acceleration of the capsubot is positive.
Phase II: In this phase, acceleration of the capsubot is negative.

1. *Phase I,* $t \in [0, t_1)$:In this phase, acceleration of the capsubot is positive. To simplify, assume that $y_2=\alpha$. $t=f_1(t)$, where α is the acceleration. In order to optimize the energy consumption, we consider the following cost function in this phase:

$$J_1 = \int_0^{t_1} [((\frac{1}{2})u(t))^2 + (y_2 - \alpha t)^2]dt \Rightarrow$$
$$J_1 = \int_0^{t_1} [((\frac{1}{2})u(t))^2 + (y_2 - f_1(t))^2]dt$$

2. *Phase II,* $t \in [t_1; t_2)$: In this phase, acceleration of the capsubot is negative. To simplify, we assume that$y_2=-\beta t+\gamma=f_2(t)$, where β is acceleration and γ is the velocity at t_1. In order to optimize energy consumption, we consider the following cost function in this phase:

$$J_2 = \int_{t_1}^{t_2} [((\frac{1}{2})u(t))^2 + (y_2 + \beta t - \gamma)^2]dt \Rightarrow$$
$$J_2 = \int_{t_1}^{t_2} [((\frac{1}{2})u(t))^2 + (y_2 - f_2(t))^2]dt$$

We assume that the capsubot velocity is zero at the end of this phase ($t = t_2$).

3.2 Stationary mode, $t \in [t_2; t_3)$:

In this stage, optimization is not an objective; however, the following conditions are satisfied:

- Inner mass returns to the initial condition.
- Capsubot during this mode does not move.

This mode includes four phases as follows [5]:

Phase I, $t \in [t_2; t_{21})$: In this phase, $\dot{y}_3 < 0$ and $0 < \dot{y}_4 \le a_m$ which indicates small backward decelerated motion of the inner mass.
Phase II, $t \in [t_{21}; t_{22})$: In this phase, $\dot{y}_3 > 0$ and $0 < \dot{y}_4 \le a_m$ which means small forward accelerated motion of the inner mass.
Phase III, $t \in [t_{22}; t_{23})$: In this phase, $\dot{y}_3 = v_0$ and $\dot{y}_4 = 0$ which illustrates uniform motion of the inner mass with a small velocity.
Phase IV, $t \in [t_{23}; t_3)$: In this phase, $\dot{y}_3 > 0$ and $-a_m \le \dot{y}_4 < 0$ which means small forward accelerated motion of the inner mass.

a_m is the maximal acceleration of the inner mass where the capsubot shell remains stationary. Here, V_0anda_m in the stationary mode have been calculated in [4].

4. Control design

The sign-function used in (5) is not continuous which creates difficulties in differentiation and solving the optimal control problem. Therefore, we use the function $tanh(y/\varepsilon)$, $\varepsilon \to 0$, instead.

A control input u is chosen so that it minimizes the following objective function:

$$J(u) = h(y(t_f), t_f) + \int_{t_0}^{t_f} g(y(t), u(t), t)dt$$

where t_0 and t_f are the initial and final time; h and g are scalar functions.

The system state equations are as follows:

$$\dot{y}(t) = a(y(t), u(t), t)$$

Using the Hamiltonian definition [11] we can write

$$\begin{aligned} &\mathrm{H}(y(t), u(t), p(t), t) = g(y(t), u(t), t) \\ &+p^T(t)[a(y(t), u(t), t)] \end{aligned} \tag{6}$$

where $p(t)$ is a vector of costate variables of the same dimension as the state variables $y(t)$, and costate variables are part of the solution.

Using (5) and (6) we can obtain

$$\begin{aligned} &\lim_{\varepsilon \to 0} \mathrm{H}(y(t), u(t), p(t), t) = \frac{1}{2}u^2(t) + (y_2 - f_i(t))^2 \\ &+p_1(t)y_2 + p_2(t)\{-\frac{\mu_{1k}}{M}(M+m)g.\tanh(\frac{y_2}{\varepsilon}) \\ &+\frac{\mu_{2k}}{M}mg.\tanh(\frac{y_4 - y_2}{\varepsilon}) + \frac{1}{M}u\} \\ &+p_3(t)y_4 + p_4(t)\{-\mu_{2k}g.\tanh(\frac{y_4 - y_2}{\varepsilon}) - \frac{1}{m}u\} \\ &i = 1, 2 \end{aligned} \tag{7}$$

The necessary condition for optimality can be obtained as

$$\begin{cases} \dot{y}^*(t) = \dfrac{\partial \mathrm{H}}{\partial p}(y^*(t), u^*(t), p^*(t), t) \\ \dot{p}^*(t) = -\dfrac{\partial \mathrm{H}}{\partial y}(y^*(t), u^*(t), p^*(t), t) \\ 0 = \dfrac{\partial \mathrm{H}}{\partial u}(y^*(t), u^*(t), p^*(t), t) \end{cases} \tag{8}$$

where ($t \in [t_0; t_f)$) boundary conditions are as follows:

$$[\frac{\partial h}{\partial y}(y^*(t_f),t_f)-p^*(t_f)]^f \delta y_f + [H(y^*,u^*,p^*,t_f)+\frac{\partial h}{\partial t}(y^*(t_f),t_f)]\delta t_f = 0 \quad (9)$$

Therefore, the necessary conditions and boundary conditions for the first stage are obtained as follows:

$$\begin{cases} \dot{y}_1^* = y^*_2 \\ \dot{y}_2^* = -\frac{\mu_{1k}}{M}(M+m)g.\tanh(\frac{y^*_2}{\varepsilon}) + \frac{\mu_{2k}}{M}mg.\tanh(\frac{y^*_4 - y^*_2}{\varepsilon}) + \frac{1}{M}u \\ \dot{y}_3^* = y^*_4 \\ \dot{y}_4^* = -\mu_{2k}g.\tanh(\frac{y^*_4 - y^*_2}{\varepsilon}) - \frac{1}{m}u \end{cases} \quad (10)$$

Hence, we let

$$\dot{p}^*_1(t) = -\frac{dH}{dy_1} = 0$$

$$\dot{p}^*_2(t) = -\frac{dH}{dy_2} = -p^*_1(t) - 2\times(y_2 - f_i(t)) + p^*_2(t)\times\frac{\mu_{1k}}{M}(M+m)g\times\frac{1}{\varepsilon(1+\cosh^2(\frac{y_2}{\varepsilon}))} - p^*_2(t)\times\frac{\mu_{2k}}{M}mg\times\frac{-1}{\varepsilon(1+\cosh^2(\frac{y_4-y_2}{\varepsilon}))} + p^*_4(t)\times\mu_{2k}g\times\frac{-1}{\varepsilon(1+\cosh^2(\frac{y_4-y_2}{\varepsilon}))}$$

$$\dot{p}^*_3(t) = -\frac{dH}{dy_3} = 0$$

$$\dot{p}^*_4(t) = -\frac{dH}{dy_4} = -p^*_2(t)\times\frac{\mu_{2k}}{M}mg\times\frac{-1}{\varepsilon(1+\cosh^2(\frac{y_4-y_2}{\varepsilon}))} - p^*_3(t) + p^*_4(t)\times\mu_{2k}g\times\frac{-1}{\varepsilon(1+\cosh^2(\frac{y_4-y_2}{\varepsilon}))}$$

$$\frac{dH}{du} = u^* + p^*_2(t)\times\frac{1}{M} - p^*_4(t)\times\frac{1}{m} = 0$$

$$\Rightarrow u^* = p^*_4(t)\times\frac{1}{m} - p^*_2(t)\times\frac{1}{M}$$

$$[\frac{\partial h}{\partial y}(y^*(t_f),t_f)-p^*(t_f)]^T \delta y_f + [H(y^*,u^*,p^*,t_f)+\frac{\partial h}{\partial t}(y^*(t_f),t_f)]\delta t_f = 0$$

$$i = 1,2$$

The above nonlinear equations are solved by numerical methods (run in MATLAB Ver.7.12.0.635).

In stage 2, the partial feedback linearization control approach is used [4]. So, in stationary mode the desired velocity of the inner mass ($\dot{y}_{3d}(t)$) can be written as [5]:

$$\dot{y}_{3d}(t) = y_{4d}(t) = \begin{cases} \frac{v_1(t-t_{21})}{t_{21}-t_2} & t\in[t_2,t_{21}) \\ \frac{v_0(t-t_{21})}{t_{22}-t_{21}} & t\in[t_{21},t_{22}) \\ v_0 & t\in[t_{22},t_{23}) \\ \frac{v_0(t_3-t)}{t_3-t_{23}} & t\in[t_{23},t_3) \end{cases}$$

For calculating the parameters in the desired velocity profile, we have

- ***v_1 and t_{21}:***

Due to the continuity in the velocity of the inner mass, we can write

$$\frac{v_1(t-t_{21})}{t_{21}-t_2}\Big|_{t=t_2} = \dot{y}_3(t_2) \Rightarrow v_1 = -\dot{y}_3(t_2)$$

and

$$\frac{d}{dt}\left(\frac{v_1(t-t_{21})}{t_{21}-t_2}\right) = a_m \Rightarrow t_{21} = \frac{1}{a_m}(v_1 + a_m t_2)$$

- ***t_{22}:***

$$\frac{d}{dt}\left(\frac{v_0(t-t_{21})}{t_{22}-t_{21}}\right) = a_m \Rightarrow t_{22} = \frac{1}{a_m}(v_0 + a_m t_{21})$$

- ***t_3 and t_{23}:***

$$\frac{d}{dt}\left(\frac{v_0(t_3-t)}{t_3-t_{23}}\right) = -a_m \Rightarrow t_3 = \frac{1}{a_m}(v_0 + a_m t_{23})$$

In this phase, the maximal deceleration (**$-a_m$**) is used.

The initial and final velocity of the inner mass are ω_0 and zero respectively. In phase II, the maximal acceleration (a_m) is used. The initial and final velocity of the inner mass are zero and v_0 respectively. So we can write

$$t_3 - t_{33} = t_{32} - t_{31} \Rightarrow t_{33} = t_3 - t_{32} + t_{31}$$

So, from (5), we can write

$$\dot{y}_4 = -\frac{1}{m}u - \mu_{2k}g.\mathrm{sign}(y_4 - y_2) \Rightarrow \dot{y}_4 = -\frac{1}{m}u - \mu_{2k}g.\mathrm{sign}(\dot{y}_3 - \dot{y}_1) \quad (11)$$

Using the partial feedback linearization control approach, the control law can be selected as follows [16]:

$$u = \alpha\tau' + \beta \quad (12)$$

where u is the input force. We choose

$$\alpha = -m$$
$$\beta = -\mu_{2k} m.g.\text{sign}(\dot{x}_2 - \dot{x}_1)$$

Let $E = y_3 - y_{3d}$ be the tracking error; choosing

$$\tau' = \dot{y}_{4d} - k_v(\dot{y}_3 - \dot{y}_{3d}) - k_p(y_3 - y_{3d}) \Rightarrow$$
$$\tau' = \dot{y}_{4d} - k_v(y_4 - y_{4d}) - k_p(y_3 - y_{3d}) \quad (13)$$

Applying (13) to (11) gives the error equation; it is quite easy to show that the closed-loop system is characterized by the error equation

$$\ddot{E} + k_v\dot{E} + k_pE = 0 \quad (14)$$

The value of k_v and k_p can be selected such that the inner mass tracks the desired trajectory profile.

5. Simulation results

In this section, capsubot movement is simulated in two cases. In Case 1, Open-Loop Control (OLC) and Close-Loop Control (CLC) are used with parameters given in [14] and in Case 2, the proposed optimal control strategy is used. In this paper, it is supposed that the static friction coefficient is about twice the kinetic friction coefficient. Thus, $\mu_{1s}=2\mu_{1k}$and $\mu_{2s}=2\mu_{2k}$are used in the model for simulation [13]. The simulation is carried out using MATLAB Ver.7.12.0.635 for $Ts = 1ms$. The parameters used for the optimal control approach in this paper are given in Table 1where the common parameters are taken from [14].

M(kg) Capsubot mass	m(kg) Inner mass	μ_{1s}(N/m/s)	μ_{2s}(N/m/s)
0.9	0.6	0.166	0.016
a_m(m/s²)	v_0(m/s)	v_1(m/s)	t_1(s)
2.034	0.2	0.7343	0.4
t_2(s)	t_{21}(s)	t_{22}(s)	t_{23}(s)
0.572	0.933	1.01314	3.2
t_3(s)	α(m/s²)	β(m/s²)	γ(m/s)
3.2983	0.55	-1.4544	0.71267

Table 1. Parameters of the simulated capsubot system.

To compare the OLC, CLC [4], and the optimal control approaches with each other, we must consider the same displacement for them. Because the capsubot displacement in the OLC and CLC approaches are the same, we use a figure to depict displacement of the capsubot in CLC and OLC. So Fig. 2shows the capsubot motion in one cycle using OLC and CLC, and Fig.3 shows the capsubot motion in three cycles using optimal control.

As depicted in Fig.2 and Fig.3, the amount of displacement using the OLC and CLC approaches are equal to the optimal control approach in the same time interval.

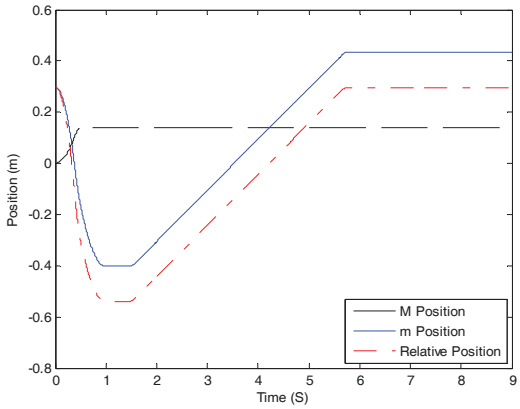

Figure 2. Trajectories of the capsubot positions in one cycle using OLC and CLC.

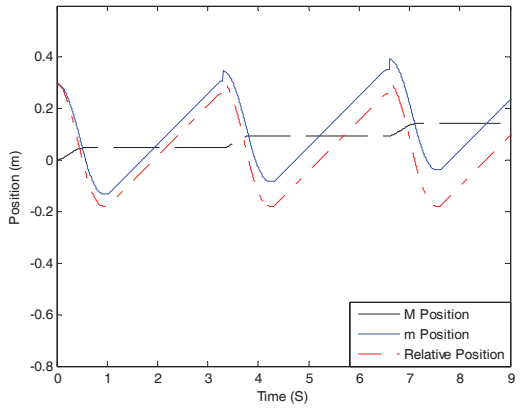

Figure 3. Trajectories of the capsubot positions in three cycles using optimal control.

Fig.4 and Fig.5 illustrate the capsubot velocity and the inner mass velocity respectively using both OLC and CLC approaches. Fig.6 and Fig.7 show the capsubot velocity and the inner mass velocity respectively using optimal control.

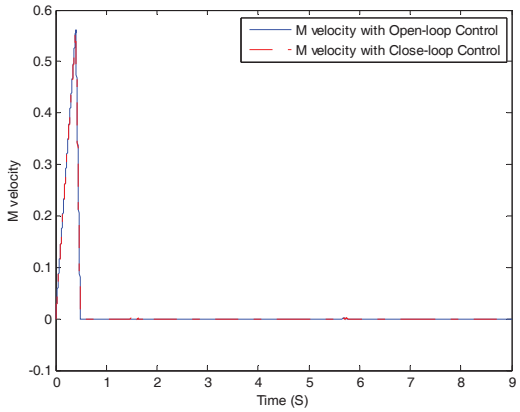

Figure 4. The capsubot velocity in one cycle using OLC and CLC.

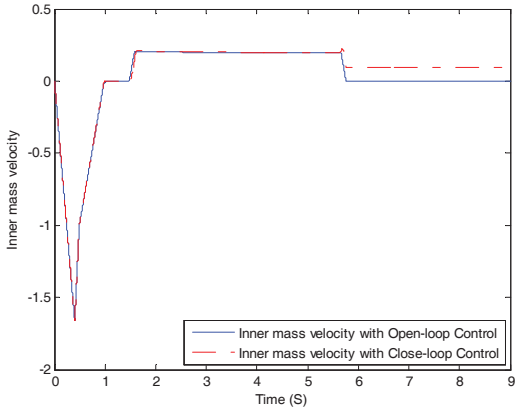

Figure 5. The inner mass velocity in one cycle using OLC and CLC.

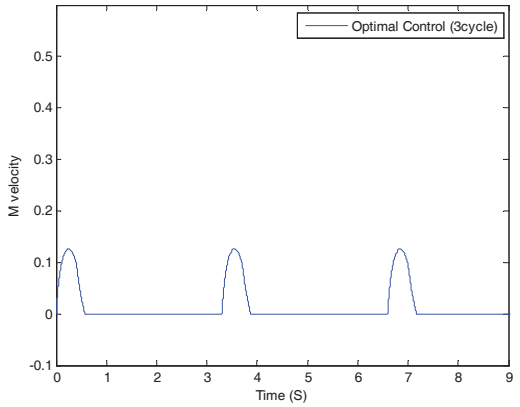

Figure 6. The capsubot velocity in three cycles using optimal control.

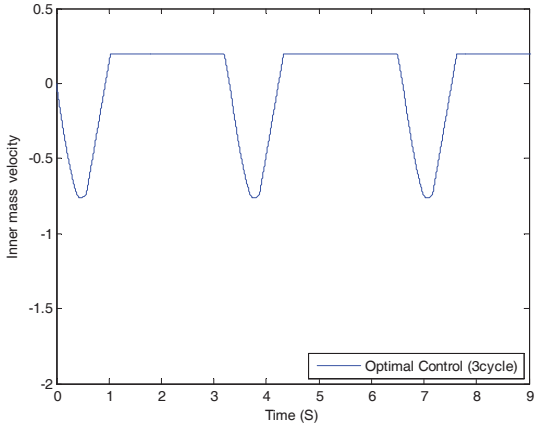

Figure 7. The inner mass velocity in three cycles using optimal control.

Comparing the performances of these three controllers for the same displacement, it is obvious that the capsubot and the inner mass velocities using the optimal control approach are smoother than the OLC and CLC approaches. In addition, the absolute peaks in the former approaches are more than the latter one.

The forces generated by piezoelectric element in OLC, CLC and optimal control are shown in Fig.8, Fig.9 and Fig.10, respectively.

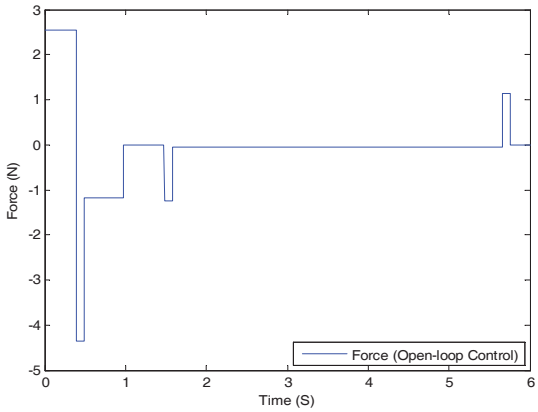

Figure 8. Force used in the OLC in one cycle.

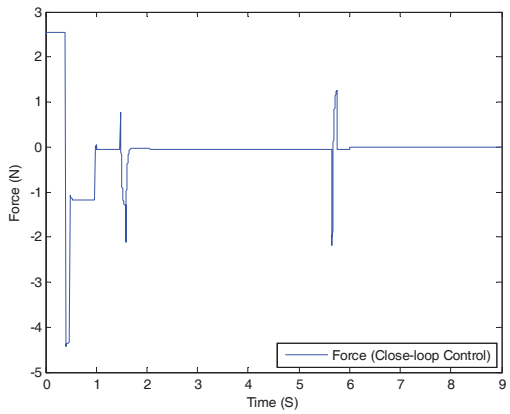

Figure 9. Force used in the CLC in one cycle.

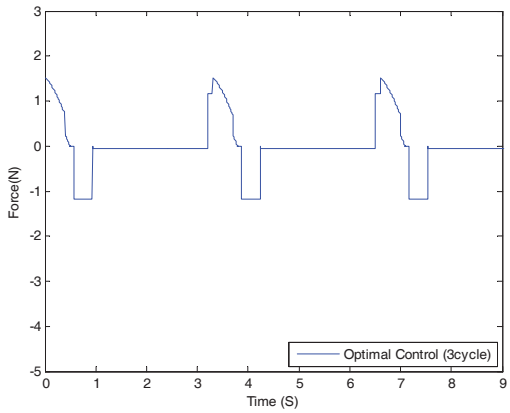

Figure 10. Force used in the optimal control in three cycles.

Energy consumption can be calculated as follows:

$$W = \int_0^{L_f} |F| . d\ell \approx \sum_{i=0}^{N} |F_i| . \Delta\ell_i$$

where L_f is final position of the capsubot. We can see that, energy consumption for the same displacement in the OLC, CLC and optimal control approaches are 0.3968J, 0.3932J and 0.1363J, respectively. Additionally, the absolute peak of force input in OLC is 4.35N, in CLC is 4.4158N and in optimal control is 1.5188N. So we can use a cheaper piezoelectric element as an actuator.

6. Conclusions

This paper presented an optimal control approach for the capsobut system. Simulation results show a significant improvement in smoothness and energy consumption in the proposed approach leading to selection of cheaper piezoelectric element as an actuator.

Further work on this field includes robust control with parameter uncertainty and disturbance, adaptive control with extended parameter uncertainty, and testing of the device in a real complex environment.

7. References

[1] T. Bakker, K. Asselt, J. Bontsema, J. Muller and G. Straten, A path following algorithm for mobile robots, Autonomous Robots, vol. 29, no. 1, pp. 85-97, 2010.

[2] H. Rezaee and F. Abdollahi, Mobile robots cooperative control and obstacle avoidance using potential field, in Proceedings of the IEEE/ASME International Conference on Advanced Intelligent Mechatronics (AIM), Hungary, pp. 1-66, July 2011.

[3] H. Rezaee and F. Abdollahi, A synchronization strategy for three dimensional decentralized formation control of unmanned aircrafts, in Proceedings of the IEEE Industrial Electronics Society Conference (IECON), Australia, November 2011.

[4] Y. Liu, H. Yu and T. C. Yang, Analysis and control of a capsubot, in Proceedings of the 17th IFAC World Congress, pp. 756-761, Korea, July 2008.

[5] Y. Liu and H. Yu, Variable structure control of a capsule robot system, in Proceedings of the IEEE International Conference on Networking, Sensing and Control, pp. 220226, Japan, March 2009.

[6] G. Kosa, M. Shoham and M. Zaaroor, Propulsion of a Swimming Micro Medical Robot, in Proceedings of the IEEE International Conference on Robotics and Automation, pp. 1327-1331, Spain, April 2005.

[7] M. E. Karagozler, E. Cheung, K. Jiwoon and M. Sitti, Miniature Endoscopic Capsule Robot using Biomimetic Micro Patterned Adhesives, in Proceedings of the 1st IEEE/RAS-EMBS International Conference on Biomedical Robotics and Biomechatronics, pp. 105-111, Italy, February 2006.

[8] C. Stefanini, A. Menciassi and P. Dario, Modeling and Experiments on a Legged Microrobot Locomoting in a Tubular, Compliant and Slippery Environment, International Journal of Robotics Research, pp. 551-560, May 2006.

[9] H. Li, K. Furuta and F. L. Chernousko, Motion Generation of the Capsubot using Internal Force and Static Friction, in Proceedings of the 45th IEEE Conference on Decision and Control, pp. 6575-6580, USA, December 2006.

[10] B. Kim, S. Park, C. Y. Jee and S. J. Yoon, An Earthworm-like Locomotive Mechanism for Capsule Endoscopes, in Proceedings of IEEE/RSJ International Conference on Intelligent Robots and Systems, pp. 2997-3002, South Korea, August 2005.

[11] D. E. Kirk, Optimal Control Theory An Introduction, Prentice-Hall, Englewood Cliffs, New Jersey, USA, 1970.

[12] N. Lee, N. Kamamichi, J. Ishikawa and K. Furuta, Positioning control of a capsule robot using sliding mode control, IEEE International Conference on Robotics and Biomimetics (ROBIO), pp. 995-1000, China, December 2009.

[13] Y. Liu, H. Yu and L. Vladareanu, An Iterative Learning Control Scheme for the Capsubot, in Proceedings of the UKACC International Conference on Control, UK, September 2008.

[14] W. Chen, M. Fang and H. Yu, Model Predictive Control Applied into Time Delay Capsubot System, International Conference on Intelligent Human-Machine Systems and Cybernetics, pp. 112115, China, August 2009.

[15] H. Yu, N. Huda and S. O. Wane, A novel acceleration profile for the motion control of capsubots, in Proceedings of the IEEE International Conference on Robotics and Automation, pp. 2437-2442, China, May 2011.

[16] J. J. Craig, Introduction to Robotics Mechanics and Control, Addison Wesley Longman Publishing Company, Inc, USA, 1989.